nature structural & molecular biology

# Capped small RNAs and *MOV10* in human hepatitis delta virus replication

Dirk Haussecker, Dan Cao, Yong Huang, Poornima Parameswaran, Andrew Z Fire & Mark A Kay

**The evolutionary origin of human hepatitis delta virus (HDV) replication by RNA-directed transcription is unclear. Here we identify two species of 5′-capped, ~18–25-nucleotide small RNAs. One was of antigenomic polarity, corresponding to the 5′ end of hepatitis delta antigen (HDAg) mRNA, and interacted with HDAg and RNA polymerase II (Pol II), whereas the other mapped to a structurally analogous region on the genomic RNA hairpin. An HDAg-interaction screen indicated that HDAg interacts with MOV10, the human homolog of the *Arabidopsis thaliana* RNA amplification factor gene *SDE3* and *Drosophila melanogaster* RISC-maturation factor gene *Armitage* (*armi*). *MOV10* knockdown inhibited HDV replication, but not HDAg mRNA translation, further supporting a role for MOV10 in RNA-directed transcription. Together, our studies define RNA hairpins as critical elements for the initiation of HDV-related, RNA-directed transcription. The identification of capped small RNAs and the involvement of MOV10 in HDV replication further suggest a conserved mechanism related to RNA-directed transcription in lower eukaryotes.**



RNA-directed transcription is the generation of an RNA transcript from an RNA template and is carried out by RNA-dependent RNA polymerases (RdRPs). RNA-directed transcription is known from RNA interference (RNAi)-related amplification of gene silencing in non-vertebrate species such as *Caenorhabditis elegans*, fungi and plants[1]. It is also part of the replication cycle of vertebrate RNA viruses. For the majority of viruses, these processes are carried out by virally encoded RdRPs. There are, however, two known exceptions: plant viroids and HDV (for a review of HDV replication, see ref. 2).

HDV is the smallest known animal virus and encodes only one protein, the hepatitis delta antigen (HDAg). Because HDAg does not have polymerase activity, HDV relies on host RNA polymerases to amplify its RNA genome. This is remarkable because nonviral, cellular RNA–directed transcription is otherwise thought to be absent in vertebrates. This raises the question of whether HDV replication uses an independently evolved RNA-directed transcription process or a more general and ancient capacity for RNA-directed transcription[3]. In this context, the presence of *MOV10* and *Armitage* in the human and fly genomes, respectively, is notable. *MOV10* and *Armitage* are the homologs of *A. thaliana SDE3*, which encodes a putative RNA helicase that had originally been isolated as the first non-RdRP factor required for the amplification step of RNAi in plants[4]. *SDE3* is required for single-strand RNA-induced RNAi, but dispensable for hairpin RNA-induced RNAi. *Drosophila* Armitage has been shown to act as a maturation factor during RISC assembly[5]; human MOV10 is associated with Argonaute proteins, but its role in RNA silencing is unclear[6].

Infectious HDV particles are packaged with hepatitis B surface antigen (HBsAg), restricting the virus's infection and spread to people with HBV. Once inside a mammalian cell, HDV replication requires only HDV RNA and a source of HDAg[2]. After infection, the circular genomic HDV RNA reaches the nucleus, where it becomes the template for rolling-circle replication, thus generating multimers of antigenomic HDV RNAs. The multimers are cleaved into monomers by a ribozyme activity in the antigenomic RNA, which then circularize by end-ligation. Antigenomic RNA, in turn, becomes the template for analogous rolling-circle replication, thereby yielding more genomic HDV RNAs. Because they have >70% intramolecular Watson-Crick base-pair complementarity, both genomic and antigenomic HDV RNAs assume a compact, unbranched, rod-like structure. HDAg mRNA is capped and polyadenylated and therefore is most likely generated by Pol II. Partly owing to the circular nature of full-length antigenomic and genomic HDV RNA, the HDAg mRNA 5′ end is also the only defined 5′ end of an HDV RNA indicative of transcription initiation[7–9]; the initiation sites for full-length antigenomic and, particularly, genomic HDV RNA have not been determined. Although it had been speculated that Pol I may mediate full-length antigenomic HDV RNA synthesis[10], recent nuclear run-on[11] and HDV RNA immunoprecipitation[12] studies favor a model in which the core Pol II enzyme mediates all HDV RNA synthesis.

The evolutionary origin and molecular details of HDV-related RNA-directed transcription, including its initiation and associated non–Pol II host factors, remain largely unknown. We hypothesized that HDV might compensate for its limited coding capacity by using noncoding small RNAs similar to the ones implicated in RNAi-related processes[13]. Such an RNA may function either in modulating viral or host transcript levels by RNA silencing and/or in the initiation of RNA-directed transcription, possibly similar to the RdRP-dependent triphosphorylated small RNAs in *C. elegans* RNA silencing[14].

Departments of Pediatrics and Genetics, Stanford University, 300 Pasteur Dr., Rm. G305, Stanford, California 94305, USA. Correspondence should be addressed to M.A.K. (markay@stanford.edu).

Received 15 February; accepted 8 May; published online 15 June; corrected online 22 June 2008; doi:10.1038/nsmb.1440

## RESULTS

### A capped HDV small RNA related to the HDAg mRNA 5′ end

The pre-microRNA-like appearance of the folded genomic and antigenomic HDV RNA hairpin ends ('pode' and 'antipode') prompted us to probe for small RNAs corresponding to either the top or the bottom strands of these hairpins (**Fig. 1a**,**b**). In this initial northern-blotting screen, we detected an HDV-derived and replication-dependent small RNA with an oligonucleotide probe targeting the bottom strand of the antigenomic pode (**Fig. 1b**, boxed). This ~24–25-nt RNA was observed in both HDV-replicating Huh-7 (**Fig. 1c**, lanes 1–3) and 293 (lanes 4–7) cells, regardless of whether HDV replication had been induced by plasmid or RNA transfection (**Fig. 1c**, lanes 5 and 7). Transfection with a plasmid that contains an early nonsense mutation in HDAg, and that consequently does not support HDV replication, did not result in such small RNAs (**Fig. 1c**, lanes 2 and 6). We therefore consider this RNA to be a *bona fide* HDV small RNA.

To more precisely map the small RNA, we used a primer-extension assay specific for detecting the 5′ end of the small RNA, but not that of the collinear, approximately 800-nt HDAg mRNA (**Fig. 1d**,**e**). The HDAg mRNA 5′ end is the only established 5′ end of an HDV RNA and had been mapped to positions 1630 and 1631 (refs. 7–9). We therefore used RNA preparations depleted of molecules larger than 200 nucleotides (nt) (Methods). As a negative control, we chose a primer that should anneal downstream of the predicted HDV small RNA, but that would still anneal to HDAg mRNA. We initially chose an HDV small RNA–directed primer of which the 3′ end was at position 1627 and obtained a 3–4-nt extension that was seen only in the HDV-containing samples (data not shown). Confirming the specificity of these results, a primer shortened by 2 nt at the 3′ end yielded a ~5–6-nt extension (**Fig. 1e**, left panel), mapping the 5′ end of the small RNA to around position 1630-1631 (**Fig. 1d**). No HDV-dependent product was seen with the negative control primer, supporting the efficient depletion of HDAg mRNA in the samples (**Fig. 1e**, right panel). We conclude that the 5′ end of the HDV small RNA coincides with that of HDAg mRNA and is within the evolutionarily conserved RNA secondary structure thought to harbor promoter activity[15].

We next determined the nature of the small RNA 5′ and 3′ ends. The 3′ end was studied with the chemical β-elimination assay[16]. The increased gel mobility after β-elimination is consistent with a 2′,3′-hydroxyl 3′ end similar to that of miR-15a (**Fig. 2a**). We investigated the 5′ end by enzymatic means (**Fig. 2b**,**c**). As for the 5′-monophosphorylated miR-15a, T4 PNK, which adds a phosphate to 5′-hydroxylated RNAs, did not affect the mobility of the HDV small RNA, excluding the possibility of a 5′-OH terminus (**Fig. 2b**, lane 3). Tobacco acid pyrophosphatase (TAP) cleaves various pyrophosphate bonds, including those in triphosphorylated and methylguanosine-capped RNAs, leaving a 5′-monophosphate group. A change from triphosphate to monophosphate has a negligible effect on the mobility of small RNAs under comparable conditions[14]; the loss of a cap,

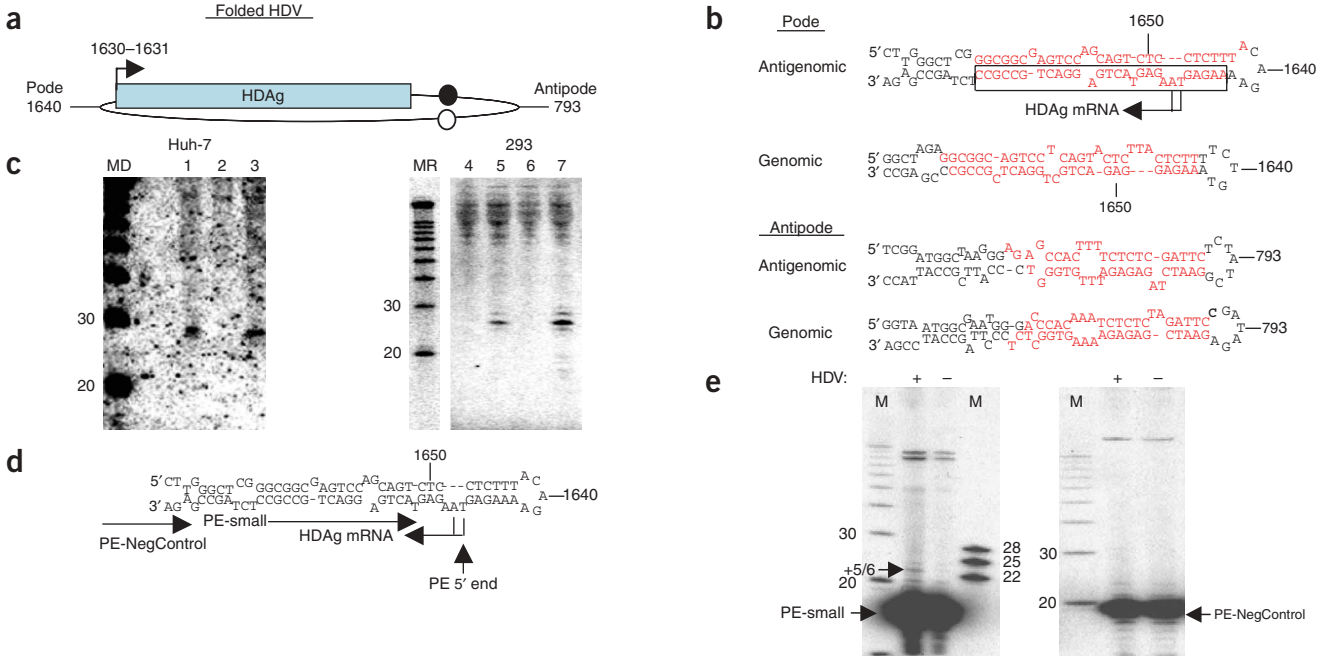


**Figure 1** Discovery and mapping of an HDV-derived small RNA. (**a**) Schematic of HDV secondary structure (applies to both genomic and antigenomic HDV RNA). HDAg, HDAg mRNA; arrow, HDAg mRNA start site. Circles, antigenomic (filled) and genomic (open) ribozymes; nucleotide numbering according to Kuo *et al.*[34]. (**b**) Predicted secondary structures of both genomic and antigenomic RNA hairpin ends. Top and bottom strands of all four hairpins were screened for corresponding small RNAs. Target sequences for the northern-blot oligonucleotide probes in this screen are marked in red, the region from which the small RNA was detected by a black box, and reported[7–9] HDAg mRNA start sites by arrows. (**c**) An HDV-derived small RNA from the antigenomic pode (northern blot). 1–3 (Huh-7, day 11): 1, DNA induction, wt HDAg; 2, DNA induction, mutant HDAg; 3, DNA induction with construct engineered to express only the small HDAg (note: only the small, but not the large, isoform of HDAg is required for HDV replication). 4–7 (293, day 6): 4, untransfected; 5, DNA induction, wt HDAg; 6, DNA induction, mutant HDAg; 7, RNA induction. MD, DNA size marker; MR, RNA size marker. (**d**,**e**) HDV small RNA 5′-end mapping by primer extension (PE). The primer extension strategy is shown in **d**. Arrows toward the left indicate the HDAg mRNA initiation site(s), and the vertical arrow the major 5′ end mapped by PE. The relative positions of the extension primers 'PE-small' and 'PE-NegControl' are indicated. In **e**, a largely 5–6-nt extension maps the HDV small RNA to positions 1630-1631. The absence of an HDV-dependent extension with 'PE-NegControl' confirms the specificity of the assay with regard to the HDV small RNA. Numbers indicate nucleotide sizes and '+(number)' the extent of the extension. HDV+, DNA induction, wt HDAg; HDV–, DNA induction, mutant HDAg; M, DNA marker (nucleotides).

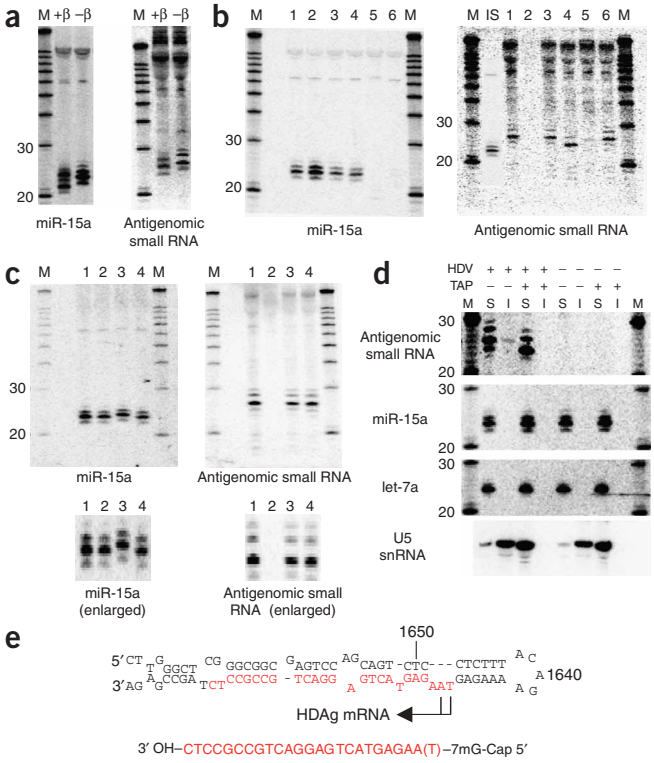


**Figure 2** The antigenomic HDV small RNA is 2′-3′-hydroxylated and has an mRNA-like 5′ cap (northern blot, 293 cells, RNA induction). (**a**) 3′ end assessed by β-elimination. The mobility of the HDV small RNA is increased after β-elimination. miR-15a, 2′-3′-hydroxylated positive control; +β, +β-elimination; −β, untreated RNA. (**b**) 5′ end assessed by enzymatic analysis. 1, mock-treated (+HDV); 2, mock-treated (no HDV); 3, PNK (+HDV); 4, decapping enzyme (TAP; +HDV); 5, T4 RNA ligase (+HDV); 6, Terminator exonuclease (+HDV). The size of the HDV small RNA was estimated to be ~24 nt based on the largely 22-nt, 5′-phosphorylated miR15-a shown in the inset (IS). (**c**) Confirmation that the 5′ end of the HDV small RNA is capped, not triphosphorylated (image enlarged to emphasize changes in gel mobility for miR-15a, but not HDV small RNA). 1, mock-treated (+HDV); 2, mock-treated (no HDV); 3, Antarctic phosphatase (+HDV); 4, Antarctic phosphatase followed by T4 PNK (+HDV). (**d**) RNA immunoprecipitation with antibody (K121) to 2,2,7-trimethylguanosine. The immunoprecipitation efficiency of the HDV small RNA, U5 snRNA (positive control) and microRNAs miR-15a and let-7a (negative controls) was analyzed by northern blotting. S, supernatant; I, immunoprecipitate fraction. (**e**) Predicted structure of the HDV small RNA. The various RNAs in **a**–**d** were detected after stripping and rehybridization to the same blot. M, RNA marker.

however, should increase small RNA mobility because of the additional loss of the guanosine moiety. Consistent with the presence of a cap, the mobility of the HDV small RNA was increased by TAP treatment (**Fig. 2b**, lane 4), whereas that of miR-15a was unchanged. The existence of a triphosphorylated end was further excluded by treatment with Antarctic phosphatase, which had no effect on HDV small RNA gel mobility (**Fig. 2c**, lane 3), neither did subsequent treatment with PNK (lane 4). By contrast, the internal control miR-15a was slightly retarded by Antarctic phosphatase and was restored to its original mobility by PNK. The disappearance of miR-15a and HDV small RNA upon treatment with T4 RNA ligase can be explained by ligation of the 3′-hydroxyl ends of the HDV small RNA to a heterogeneous population of 5′-monophosphorylated RNAs in the sample[14]. Finally, the HDV small RNA proved resistant to Terminator exonuclease, an enzyme that selectively removes 5′-monophosphorylated RNAs such as miR-15a (**Fig. 2b**, lane 6). Although these data indicated that the HDV small RNA was 5′ capped, we decided to more precisely determine its identity by performing RNA immunoprecipitation with an antibody directed against trimethylguanosine (TMG) that is known also to weakly recognize 7-methylguanosine caps[17]. Consistent with the presence of an mRNA-like monomethylguanosine cap, the precipitation efficiency of TAP-sensitive HDV small RNA was intermediate between those of the 5′-phosphorylated microRNAs (not recognized) and TMG-capped U5 snRNA (efficiently recognized; **Fig. 2d**). In conclusion, the 2′-3′ hydroxylation and 5′ cap of the HDV small RNA, in addition to its particular position within the HDV sequence, place the HDV small RNA in a position where it could be involved in HDV transcription initiation (**Fig. 2e**).

### Sequencing uncovers a corresponding genomic small RNA

As part of efforts to uncover structurally related endogenous small RNAs (unpublished data), we sequenced small RNAs, including those from HDV-replicating cells (**Supplementary Table 1** online). Importantly, five of the seven antigenomic HDV RNAs recovered as a result of a protocol that is designed to enrich for capped small RNAs (Methods) and that consequently largely depleted microRNAs (**Supplementary Table 1**), corresponded to the antigenomic small RNA (**Fig. 3a**; **Supplementary Table 1**). The sequence further supports the possibility that the small RNA starts at around position 1630, with a non-templated terminal nucleotide addition accounting for the extra nucleotide in the primer extension[7]. Notably, we also identified a second, distinct HDV small RNA, in this case of genomic polarity (**Supplementary Table 1** online), and subsequently confirmed it by northern blotting (**Fig. 3b**). This small RNA falls into the same pode hairpin as the antigenomic small RNA (**Fig. 3a**). Although the enzymatic 5′-modification analysis indicated that the genomic small RNA was predominantly capped (**Fig. 3c**), we cloned a 20–21-nt species without prior selection for capped RNAs (**Supplementary Table 1**), whereas we detected the 18–19-nt species in the 5′-cap–enriched fraction. A minor 5′-phosphorylated subpopulation would also be consistent with the partially persistent signal from the most slowly migrating genomic small RNA species after decapping (**Fig. 3c**, lane 6). We also cloned additional dispersed HDV small RNAs of both genomic and antigenomic polarity. We obtained these particularly following the 5′-ligation–independent cloning method[14], which would also pick up 5′-hydroxylated RNAs that are likely to represent RNA-turnover intermediates.

### Colocalization of complementary small and full-length RNAs

We then investigated the cellular localization of the HDV small RNAs (**Fig. 3d–f**). As previously reported, and reflecting export of the genomic HDV ribonucleoprotein (RNP) to the cytoplasm for packaging with HDAg and HBsAg into the HDV virion during an infection cycle, nuclear-cytoplasmic fractionation recovered the full-length genomic RNA, particularly the mature monomer, in both the nuclear and cytoplasmic fractions (**Fig. 3d**). Full-length antigenomic RNA, however, was enriched mainly in the nucleus, consistent with it largely serving as a nuclear replication intermediate and further indicating that the cytoplasmic fraction was reasonably free from nuclear RNA contaminants. Accordingly, control miR-15a and U6 snRNA were predominantly detected in the cytoplasmic and nuclear fractions, respectively (**Fig. 3e**). Notably, and in marked contrast to their full-length counterparts, it was the HDV small RNA of antigenomic

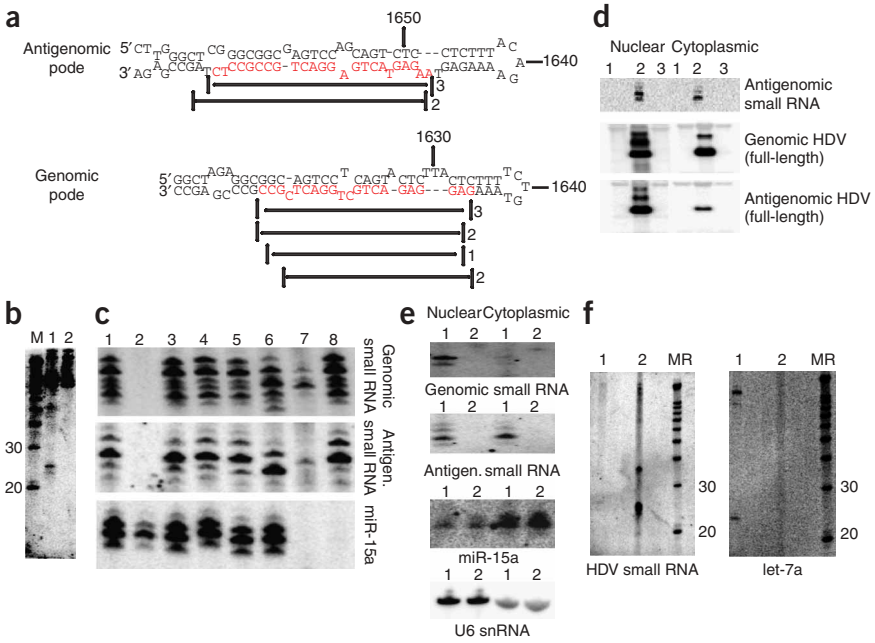


**Figure 3** Cloning and characterization of an HDV small RNA of genomic polarity. (**a**) Relative location and cloning frequency of sequenced HDV small RNAs derived from the genomic and antigenomic pode hairpins (main species highlighted in red). (**b**) Detection of genomic HDV small RNA by northern blotting (293 cells, day 5). 1, DNA induction, wt HDAg; 2, DNA induction, mutant HDAg. (**c**) Enzymatic analysis of genomic small RNA 5′ end. 1, mock-treated (+HDV); 2, mock-treated (no HDV); 3, PNK (+HDV); 4, Antarctic phosphatase (+HDV); 5, Antarctic phosphatase followed by T4 PNK (+HDV); 6, decapping enzyme (TAP; +HDV); 7, T4 RNA ligase (+HDV); 8, Terminator exonuclease (+HDV). Note that unlike the antigenomic small RNA, a minor fraction of the genomic small RNA does not appear to be shifted after TAP treatment. (**d**–**f**) Localization of the HDV small RNAs. (**d**) Nuclear-cytoplasmic fractionation of antigenomic HDV small RNA (polyacrylamide gel) and full-length antigenomic and genomic HDV RNA (denaturing agarose gel). The main species in the full-length genomic/antigenomic RNA blot corresponds to the monomer and the higher-molecular-weight species to dimer, trimer and so on. 1, DNA induction, mutant HDAg; 2, DNA induction, wt HDAg; 3, untransfected. (**e**) Genomic small RNA is restricted to the nucleus (nuclear-cytoplasmic fractionation). 1, DNA induction, wt HDAg; 2, DNA induction, mutant HDAg. miR-15a and U6 snRNA were chosen as largely cytoplasmic and nuclear RNA controls, respectively. (**f**) The HDV small RNA can be found in the HDV virion. 1, RNA induction (same RNA as in **Fig. 2c**); 2, virion RNA isolated from tissue culture media (~1.25 × $10^9$ particles). MR, RNA marker. The various RNAs in **c**–**f** were detected after stripping and re-hybridization to the same blot.



polarity that was found in both compartments, whereas the genomic small RNA was recovered only in the nuclear fraction. The colocalization of antigenomic small RNA with genomic full-length RNA, and *vice versa*, extended to the virions, where only antigenomic RNA, but neither the genomic small RNA nor the ubiquitously expressed let-7 microRNA, was readily detected (**Fig. 3f** and data not shown). Although the exact stoichiometry and biological importance of this localization remain to be determined, the ease of detection by northern blotting and preliminary quantification analysis (data not shown) are consistent with the notion that a substantial fraction of HDV virions may contain the small RNA.

## MOV10 interacts with HDAg and facilitates replication

Given their size and location within a microRNA-like precursor hairpin, we were interested in whether the HDV small RNAs had silencing activity. Dual luciferase assays with reporters carrying target sequences complementary to the HDV small RNAs in their 3′ UTR (**Supplementary Fig. 1** online and data not shown), however, did not show an HDV replication–dependent decrease in luminescence, as such an activity would have predicted. This is consistent with the HDV small RNAs being largely 5′ capped, a modification predicted to interfere with small RNA silencing[18]. An HDAg-interaction screen (HDAg immunoprecipitation followed by mass-spectrometric identification of interacting proteins; D.C., D.H and M.A.K., unpublished data) identified the human homolog of the *A. thaliana SDE3*, *MOV10* (ref. 4), both in the presence and in the absence of HDV replication (see also **Fig. 4a**). Supporting a function for MOV10 in HDV replication, *MOV10* knockdown using a pool of *MOV10*-directed siRNAs inhibited viral replication (**Fig. 4b**, lane 12). The specificity of this effect was confirmed by the fact that, in addition to the *MOV10* siRNA pool, three out of the four individual *MOV10* siRNAs tested (lanes 13–16) suppressed HDV replication, with the non-inhibitory siRNA (lane 13) showing the least *MOV10* knockdown by quantitative reverse transcriptase PCR (qRT-PCR; **Fig. 4b**). It was conceivable that *MOV10* knockdown might inhibit HDV by interfering specifically with the transcription or translation of HDAg. This possibility was of particular interest because MOV10 has been implicated in microRNA-related post-transcriptional regulation[19]. To address this, we repeated the *MOV10* inhibition experiment in cells that stably expressed HDAg and that therefore complement HDAg-mutant strains *in trans* (data not shown). *MOV10* knockdown was still sufficient to inhibit HDV replication in this cell line (**Fig. 4b**, lanes 18–20), with no obvious effect on HDAg protein levels (**Fig. 4c**). These results therefore suggest a role for MOV10 in HDV replication.

We next asked whether additional RNAi-related genes were required for HDV replication by targeting the primary microRNA processing factors DGCR8 and Drosha, the microRNA export factor exportin-5, the pre-microRNA processing enzyme Dicer and cofactor TRBP and the small RNA effector proteins Argonaute-1–4 (encoded by *AGO1–4*). In agreement with the observed lack of silencing activity of the HDV small RNAs, all of these knockdown treatments, except for one, had no appreciable effect on HDV replication, although we formally cannot rule out insufficient knockdown of these factors. The exception was Argonaute-4: all four individual siRNAs and the siRNA pool directed against *AGO4* inhibited HDV replication (**Fig. 4d**). To our knowledge, this is the first process for which a genetic requirement of *AGO4* has been identified. Because both Argonaute proteins and MOV10 have been placed at the downstream stages of microRNA silencing, it is possible that these factors function together in HDV replication.

## Interaction between small RNAs and replication factors

Considering the interaction of MOV10 with HDAg, the replication defect in *MOV10* knockdown cells, and the association of its plant

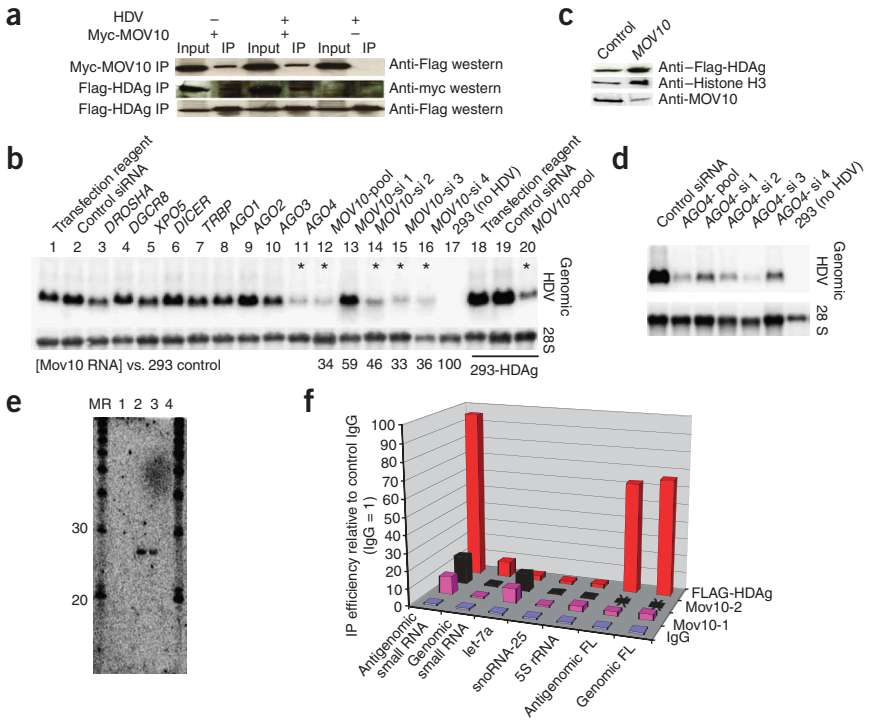


**Figure 4** Role for MOV10 in HDV replication. (**a**) Confirmation of HDAg interaction with MOV10 (immunoprecipitation analyzed by western blotting). Flag-HDAg coprecipitated with Myc-tagged MOV10, both in the presence and in the absence of HDV replication, as did Myc-MOV10 after Flag-HDAg immunoprecipitation. Owing to considerable cross-reactivity with Myc-IgG, detection of Myc-MOV10 after Myc-MOV10 immunoprecipitation was technically not feasible. IP, immunoprecipitation; Myc-MOV10 +/−, with/without co-transfected Myc-tagged MOV10; HDV +/−, protein extract from cells expressing Flag-HDAg in the presence or absence of HDV replication. HDV replication of the HDAg-mutant virus was dependent on Flag-HDAg (data not shown). (**b**) *MOV10* knockdown inhibits HDV replication (northern blot). *MOV10* knockdown with a pool (lane 12) as well as three out of four individual siRNAs (lanes 14–16) against *MOV10* inhibited HDV replication, with the noninhibitory siRNA (lane 13) showing the least effective *MOV10* knockdown as determined by qRT-PCR (3 d after siRNA transfection). Targeting of other RNAi-related proteins with pools of siRNAs did not appreciably affect HDV replication, except for *AGO4* siRNA (lane 11). Viral inhibition by *MOV10* knockdown was also observed in cells stably expressing HDAg (lanes 18–20); *, >60% HDV inhibition. (**c**) Flag-HDAg abundance in the stable cell line is not appreciably altered by *MOV10* knockdown (western blot); control and *MOV10*, control versus *MOV10* siRNA pool. (**d**) Confirmation of *AGO4* knockdown effect on HDV replication using individual *AGO4* siRNAs. (**e**,**f**) RNA immunoprecipitation. HDV RNA–containing lysate was incubated with rabbit IgG (IgG), two different antibodies to MOV10 (MOV10-1, MOV10-2; only MOV10-1 was used for full-length HDV analysis) or antibodies to Pol II and Flag, and the recovered RNA was analyzed by northern blotting (**e**) and stem-loop qRT-PCR (**f**). 1, rabbit IgG; 2, anti-Flag (HDAg); 3, anti–Pol II; 4, anti-MOV10; MR, RNA marker. Average from at least two independent experiments. FL, full-length; X, not analyzed.

homolog with RNAi-related RNA-directed transcription, we were interested in whether MOV10 also interacted with the HDV small RNAs. Northern blotting after immunoprecipitation with MOV10 antibodies did not detect the HDV small RNAs. When we used the more sensitive stem-loop qRT-PCR technique for the detection of small RNAs[20], however, both MOV10 antibodies were modestly enriched for the antigenomic small RNA (**Fig. 4e**,**f**), to a similar degree as for let-7 microRNA, and this may be consistent with an indirect interaction. By contrast, the antigenomic small RNA was readily detected after HDAg immunoprecipitation not only by qRT-PCR, but also by northern blotting (**Fig. 4e**), strongly supporting the idea that it is part of functional HDV RNP complexes. Similarly, although not as consistently as for HDAg, the antigenomic small RNA could be immunoprecipitated with an antibody against Pol II, supporting the possibility that this small RNA is closely involved in active RNA-directed transcription. The variability in the Pol II interaction could be due to a more transient interaction that is sensitive to the particular stage of viral replication at the time of extract preparation. Little association was detected for HDAg and the genomic small RNA, and none above background between either MOV10 or Pol II with the genomic small RNA (**Fig. 4f** and data not shown).

## DISCUSSION

Our studies have uncovered a new type of capped small RNAs. We consider it highly unlikely that these merely represent nonfunctional turnover intermediates of larger HDV RNA because (i) they map to corresponding genomic and antigenomic hairpin structures reported to harbor HDV promoter activity[15]; (ii) they show a distinct cellular distribution that mirrors that of their complementary full-length counterparts, possibly mediated by base-pairing; (iii) the association of the antigenomic small RNA with HDAg and Pol II suggests that the small RNA is part of functional HDV complexes; and (iv) abortive transcription initiation without further functional relevance seems at odds with the antigenomic small RNA having similar abundance in the cytoplasm and the nucleus (**Fig. 3d**). Based on qRT-PCR analyses (data not shown), there was approximately one antigenomic small RNA for every five full-length antigenomic RNAs per cell (~63,000 antigenomic small RNAs, ~326,000 antigenomic full-length copies per cell 3 d after replication initiation in 293 cells). This is a rather high ratio considering the stability of circular full-length HDV RNA[21]. There were relatively few genomic small RNAs, ~6,400 per cell, in contrast to the very high abundance of full-length genomic RNAs (~$1.68 \times 10^6$ copies per cell). The more heterogeneous nature of the genomic small RNA, as well as its limited enrichment after HDAg immunoprecipitation (**Fig. 4e**), could mean that it functions—consistent with its absence outside the nucleus—as a more transient transcription initiation intermediate.

Because post-transcriptional capping of Pol II transcripts is unknown, the capped HDV small RNAs are likely to reflect RNA-directed transcription initiation. Notably, the 5′ ends of the antigenomic small RNA and HDAg mRNA coincide, and both the antigenomic and genomic small RNAs fall within equivalent hairpin structures. Consequently, a single mode of transcription initiation, determined by hairpin structures and marked by the presence of capped small RNAs, may account for essentially all HDV RNAs present during an infection, which further suggests that antigenomic HDAg mRNA and full-length HDV RNA share a common transcription initiation site. In this model, HDAg polyadenylation would be

incompletely coupled to transcription termination, with Pol II continuing downstream to generate full-length antigenomic HDV RNA by rolling-circle transcription. Efforts, including our own (data not shown), to determine the 5′ end of full-length genomic RNA have failed. One explanation for this may be the combination of the predominantly circular nature of the genomic RNA at steady state and the challenge of analyzing highly structured RNA. It may also relate to our finding that whereas the 18–19-nt species was recovered in the 5′ cap–enriched fraction only, the 20–21-nt species, which represent 2–3-nt 3′ extensions, must have been 5′-phosphorylated in order to be cloned (**Supplementary Table 1**). Cap-dependent 5′ RACE analyses would therefore have failed to uncover the genomic transcription initiation site if the nascent 5′-capped genomic RNA were to be converted into a 5′-phosphorylated transcription initiation intermediate. The 5′-capped small RNA therefore represents the best evidence so far for the elusive genomic HDV RNA transcription initiation site.

Pol II had previously been shown *in vitro* to bind to the HDV RNA hairpins[12]. Another study reported *in vitro* HDV RNA template–dependent transcription by Pol II that was more dependent on the hairpin structure than the primary sequence[22]. In that study, the hairpin was cleaved next to a bulge proximal to the loop, with the newly generated 3′ end serving as a primer for Pol II transcription and thus resulting in an RNA with both genomic and antigenomic sequence. As this activity, in the absence of HDAg, occurred on the antipode hairpin, rather than on the pode hairpin that is thought to harbor the HDV promoter[15] and from which we detected the capped small RNAs, hairpins may have a general ability to direct the initiation of RNA-templated transcription; additional factors, such as HDAg and interacting proteins, may determine the fidelity of transcription initiation site selection during HDV replication. We note that by RT-PCR and sequencing we were able to detect a similar antigenomic pode–genomic RNA hybrid from the pode region (**Supplementary Fig. 2** online). This hybrid coimmunoprecipitated with Pol II and was the only hybrid that we detected among the four possible HDV hairpin combinations tested. Nevertheless, because nicked RNA cannot serve as a template for rolling-circle replication and efforts to visualize the hybrid by means other than PCR failed, although cleavage-extension may be an alternative mechanism for HDV transcription initiation, it probably does not account for the majority of HDV transcription.

We propose a model for HDV replication (**Supplementary Fig. 3** online) in which, after infection, the incoming viral RNA encounters the largely cytoplasmic RNA helicase MOV10, which remodels the HDV RNA into a transcription initiation–competent RNP. Once in the nucleus, Pol II binds to the pode hairpin and initiates antigenomic HDV RNA synthesis. Given that primed, but not unprimed, RNA-directed transcription initiation is readily observed *in vitro*[22,23], it is possible that an annealed small RNA would facilitate this process by serving as a small priming RNA (spRNA). This could increase the odds for a successful viral infection, particularly because early HDAg mRNA transcription is thought to be critical for replication[24].

The HDV small RNAs themselves are likely to be generated by *de novo* transcription initiation and subsequent pausing, possibly regulated by the loop. Although a fraction of the paused complexes would get elongated, some may be exported into the cytoplasm for viral packaging and/or MOV10-mediated remodeling for subsequent rounds of replication. This would be consistent with the experimental HDV replication system that we have used, which does not include a *bona fide* viral infection step, and might explain the nuclear-cytoplasmic shuttling of HDV RNP particles[25]. The exact nature of the relationship between *MOV10* and plant *SDE3*, with regard to RNA-directed transcription in general and the associated small RNAs in particular, remains to be determined.

It has been debated whether HDV-related RNA-directed transcription by a human RNA polymerase evolved independently or whether it taps into an ancient, either dormant or still active capacity for RNA-directed transcription harking back to an 'RNA World'. Our findings—of capped HDV small RNAs marking the initiation sites of HDV transcription, the requirement for the *SDE3*-related *MOV10*, and the observation that RNA-directed transcription by (*Saccharomyces cerevisiae*) Pol II *in vitro* is possible even in the absence of HDAg and solely dependent on the template structure[23]—suggest that HDV might indeed harness such a conserved mechanism. Notably, the RdRP-dependent secondary small RNAs in *C. elegans* RNAi amplification were 5′-triphosphorylated[14] and very likely generated by non-processive *de novo* transcription initiation[26]. The use of Pol II rather than a dedicated RdRP may be due to coevolution with the response of the mammalian innate immune system to double-stranded RNA and triphosphorylated 5′ ends. These are recognized as foreign and trigger innate immune responses[27].

The existence of so-called mirror-spliced antisense transcripts (MSATs) is consistent with the notion that nonviral RNA-directed transcription occurs in mammalian cells[28]. MSATs are transcripts that are the reverse complement of spliced mRNA and are best explained as having been generated by RNA-directed transcription from their corresponding mRNA. We propose that HDV may be a suitable model system for such RNA-directed transcription studies. Moreover, the discovery of nonviral capped small RNAs that can be mapped to hairpin structures and transcripts sensitive to *MOV10* inhibition may offer an opportunity to identify related spRNAs and RNA-directed transcription in mammals.

## METHODS

**Tissue culture.** To induce HDV replication by DNA transfection, we transfected Huh-7 and 293 cells with the plasmid pCMV3DCHDVx1_2ag or with variants containing either a replication-deficient HDAg mutant or a construct capable of expressing only the small isoform of HDAg. For RNA-induced replication, RNA from T7 polymerase *in vitro* transcription of BamHI-linearized pCMV3DCHDVx1_2ag and HDAg mRNA generated with the mMessage mMachine kit (Ambion) was transfected. The template for the HDAg mRNA was obtained by XbaI linearization of pcDNA3, into which the HDAg open reading frame from pCMV3DCHDVx1_2ag was cloned downstream of the T7 promoter. RNA was harvested 3–6 d (293) or 11 d (Huh) after transfection with Trizol reagent (Gibco) for total RNA, or the *mir*Vana kit (Ambion) for low-molecular-weight RNA. Medium containing $5 \times 10^8$ HDV particles per ml was kindly provided by R. Lanford (Southwest Foundation for Biomedical Research, San Antonio)[29]. 2.5 ml of medium was cleared by 2-min centrifugation at 4,000*g* and 4 °C and RNA isolated by adding 22.5 ml Trizol. The ratio of the amount of small RNAs in the virion versus the cellular RNA samples was 10–100-fold higher for the antigenomic small RNA compared to control cellular 5S rRNA, let-7 microRNA and sno25 RNA (1.2 versus 0.142, 0.019 and 0.037, respectively.

**RNAi.** 293 cells plated in 24-wells were knocked down with 12 nM (pools) or 48 nM (individual) siRNA (Dharmacon). 24 h later, HDV replication was induced by transfecting cells with 0.4 μg of pCMV3DCHDVx1_2ag. Total RNA was harvested 48 h thereafter with Trizol (Invitrogen) and analyzed by northern blotting. Actin-normalized *MOV10* RNA knockdown was assessed from the same RNA by qRT-PCR as described[30]. For primers and siRNA sequences, see **Supplementary Methods** online.

**Northern blotting.** For the detection of small RNAs, *mir*Vana (Ambion) low-molecular-weight RNA was separated by 15–20% (v/v) urea-PAGE, transferred onto Hybond-N (Amersham) nitrocellulose and hybridized to

T4 PNK–end-labeled oligo probes (see **Supplementary Methods**) at 32 °C with PerfectHyb Plus (Sigma). Blots were washed and exposed to a phosphorimager. For the detection of full-length HDV RNAs, Trizol-extracted total RNA was separated on 1% (w/v) denaturing formaldehyde-agarose gels, transferred onto Hybond-N (Amersham) nitrocellulose, and hybridized to either α-UTP-labeled, T7 polymerase–transcribed RNA from BamHI-linearized pCMV3DCHDVx1_2ag for the detection of genomic HDV RNA, or T4 PNK (NEB)-end-labeled ggcggcagtcctcagtactcttactctt for the detection of antigenomic HDV RNA.

**Primer extension.** The primer extension oligo was end-labeled with T4 PNK (NEB) and [γ-$^{32}$P]ATP (PerkinElmer). For the extension, Superscript II Reverse Transcriptase (SS2RT, Invitrogen) was employed. *mir*Vana (Ambion) low-molecular-weight RNA was annealed to the end-labeled oligo primer. Buffer, dNTP and rRNasin (Promega) were added and the reaction incubated at 42 °C for 5 min, at which point 2 μl SS2RT was added for 90 min. The reaction was terminated by heating and run out on a 20% polyacrylamide gel. Primer extension primers: 'PE-small', gcggcagtcctcagta; 'PE-NegControl', gactcggaccggctcatct.

**Analysis of small RNA 3′ and 5′ ends.** β-elimination was performed essentially as described[16]. Enzyme treatments were performed by heat-denaturing 10 μg *mir*Vana (Ambion) RNA and then adding enzyme buffer, rRNasin (Promega; except for the Terminator exonuclease treatment) and finally enzyme. 100-μl reactions (40 μl f or tobacco acid pyrophosphatase) were incubated at 37 °C (30 °C for Terminator exonuclease) for 45 min (1 h for Terminator exonuclease), acid phenol/chloroform extracted, ethanol precipitated and analyzed by northern blotting.

**RNA immunoprecipitation.** For the immunoprecipitation of capped RNAs, 20 μl of K121 beads were incubated with 10 μg of low-molecular-weight RNA by rotation in IP buffer (0.01% (w/v) SDS, 1% (v/v) Triton X-100, 1.2mM EDTA, pH 8.0, 16.7 mM Tris-HCl, pH 8.0, 167 mM NaCl). The beads were washed and the eluted RNA analyzed by northern blotting. For the detection of the antigenomic-genomic hybrid RNA, small RNA, protein-protein immunoprecipitations and *MOV10* RNAi, a stable 293 cell line was established expressing functional Flag-tagged HDAg (D.C., D.H and M.A.K., unpublished data). HDV replication was induced by transfecting these cells with the HDAg mutant version of pCMV3DCHDVx1_2ag or T7 *in vitro* transcribed RNA from the same BamHI-linearized plasmid. Lysate was prepared as described[31] and 5 μg antibodies added (see **Supplementary Methods**).

For the detection of antigenomic-genomic hybrid RNA, real-time RT-PCR was performed as described[30]. Quantification of small RNAs was done by stem-loop qRT-PCR[20]. To test the specificity of the assay for the detection of the small RNA, but not other HDV RNA species of the same polarity, we (i) confirmed the HDV replication–dependent cDNA product by sequencing and (ii) included a forward PCR primer designed to anneal upstream of the small RNA 5′ end; this did not yield a PCR product, showing that the RT-PCR was not amplifying a longer RNA sharing the same 3′ end with the HDV small RNA. For primers, see **Supplementary Methods**.

**Small RNA quantification.** Three days after induction of 293 cells with pCMV3DCHDVx1_2ag, total RNA was isolated and small RNA quantified by qRT-PCR as described for RNA immunoprecipitation above, except that, to generate an absolute standard curve, predetermined amounts of *in vitro*–transcribed HDV small RNAs were added to untreated 293 RNA for RT-PCR.

**Nuclear-cytoplasmic RNA fractionation.** Cells scraped from a 10-cm dish were first pelleted and then resuspended in 500-μl lysis buffer (0.14 M NaCl, 1.5 mM $MgCl_2$, 10 mM Tris-HCl, pH 7.5, 0.5% (v/v) Nonidet P-40) and left on ice for 10 min. Nuclei were gently pelleted by centrifugation at 3,000*g* for 2 min at 4 °C. For cytoplasmic RNA, the supernatant was underlaid with an equal volume of lysis buffer containing 12% (w/v) sucrose and spun at 15,800*g* for 10 min. The supernatant (cytoplasmic fraction) was then phenol/chloroform extracted and ethanol precipitated. For nuclear RNA, nuclei were resuspended in 1 ml of lysis buffer and gently spun down at 3,000*g* for 2 min, and the RNA was extracted from the pellet with Trizol.

**Small RNA sequencing.** *mir*Vana (Ambion) low-molecular-weight RNA was adapted as we have described in previous work[32] for the 5′-phosphate–dependent cloning, and as described by others[14] for the 5′-ligation–independent cloning. To preferentially clone capped small RNAs, the RNA was treated first with Antarctic phosphatase and then with tobacco acid pyrophosphatase before 5′-phosphate–dependent cloning. Samples were cloned as part of a barcoded pool and sequenced using the 454/Roche GS20 sequencing platform[33].

**Western blotting.** Western blotting was performed according to standard protocols. Antibodies: monoclonal anti–Flag M2 (Sigma, A8592); rabbit MOV10-2 (Protein Tech Group, 10370-1-AP); rabbit histone H3 dimethyl K4 (Abcam, ab7766).

**Dual luciferase assay.** The Dual-Luciferase Reporter (DLR) Assay (Promega) was performed according to the manufacturer's instructions, with modifications as described in the **Supplementary Methods**.

For detailed methods, see **Supplementary Methods**.

*Note: Supplementary information is available on the Nature Structural & Molecular Biology website.*

ACKNOWLEDGMENTS

We thank J. Glenn (Stanford University) for reagents, R. Lanford (Southwest Foundation for Biomedical Research, San Antonio) for HDV virions and A. Guzzetta (Stanford University) for mass spectrometry. This work was supported by grants DK78424 and AI71068 from the National Institutes of Health (to M.A.K.), a Helen Hay Whitney Foundation Postdoctoral Research Fellowship to D.C. and a Stanford Dean's Postdoctoral Fellowship to D.H.

AUTHOR CONTRIBUTIONS

D.H. designed and performed the majority of the experiments. D.C. did the proteomic screens and contributed to the immunoprecipitation experiments. Y.H. assisted D.H. in performing the experiments. P.P. did the small RNA sequencing. A.Z.F. provided input on sequencing strategies and suggestions in experimental design. M.A.K. served as supervisor and provided scientific input to experimental design and data interpretation. D.H. wrote the manuscript with input from D.C., P.P., A.Z.F. and M.A.K. All authors approved the final manuscript.

Published online at http://www.nature.com/nsmb/
Reprints and permissions information is available online at http://npg.nature.com/reprintsandpermissions/

1. Wassenegger, M. & Krczal, G. Nomenclature and functions of RNA-directed RNA polymerases. *Trends Plant Sci.* **11**, 142–151 (2006).
2. Taylor, J.M. Structure and replication of hepatitis delta virus RNA. *Curr. Top. Microbiol. Immunol.* **307**, 1–23 (2006).
3. Macnaughton, T.B. & Lai, M.M. HDV RNA replication: ancient relic or primer? *Curr. Top. Microbiol. Immunol.* **307**, 25–45 (2006).
4. Dalmay, T., Horsefield, R., Braunstein, T.H. & Baulcombe, D.C. SDE3 encodes an RNA helicase required for post-transcriptional gene silencing in *Arabidopsis*. *EMBO J.* **20**, 2069–2078 (2001).
5. Tomari, Y. *et al.* RISC assembly defects in the *Drosophila* RNAi mutant armitage. *Cell* **116**, 831–841 (2004).
6. Meister, G. *et al.* Identification of novel argonaute-associated proteins. *Curr. Biol.* **15**, 2149–2155 (2005).
7. Hsieh, S.Y., Chao, M., Coates, L. & Taylor, J. Hepatitis delta virus genome replication: a polyadenylated mRNA for delta antigen. *J. Virol.* **64**, 3192–3198 (1990).
8. Modahl, L.E. & Lai, M.M. Transcription of hepatitis delta antigen mRNA continues throughout hepatitis delta virus (HDV) replication: a new model of HDV RNA transcription and replication. *J. Virol.* **72**, 5449–5456 (1998).
9. Gudima, S., Dingle, K., Wu, T.T., Moraleda, G. & Taylor, J. Characterization of the 5′ ends for polyadenylated RNAs synthesized during the replication of hepatitis delta virus. *J. Virol.* **73**, 6533–6539 (1999).
10. Macnaughton, T.B., Shi, S.T., Modahl, L.E. & Lai, M.M. Rolling circle replication of hepatitis delta virus RNA is carried out by two different cellular RNA polymerases. *J. Virol.* **76**, 3920–3927 (2002).
11. Chang, J., Nie, X., Chang, H.E., Han, Z. & Taylor, J. Transcription of hepatitis delta virus RNA by RNA polymerase II. *J. Virol.* **82**, 1118–1127 (2007).
12. Greco-Stewart, V.S., Miron, P., Abrahem, A. & Pelchat, M. The human RNA polymerase II interacts with the terminal stem-loop regions of the hepatitis delta virus RNA genome. *Virology* **357**, 68–78 (2006).
13. Chapman, E.J. & Carrington, J.C. Specialization and evolution of endogenous small RNA pathways. *Nat. Rev. Genet.* **8**, 884–896 (2007).

14. Pak, J. & Fire, A. Distinct populations of primary and secondary effectors during RNAi in *C. elegans*. *Science* **315**, 241–244 (2007).
15. Beard, M.R., MacNaughton, T.B. & Gowans, E.B. Identification and characterization of a hepatitis delta virus RNA transcriptional promoter. *J. Virol.* **70**, 4986–4995 (1996).
16. Hutvagner, G. *et al.* A cellular function for the RNA-interference enzyme Dicer in the maturation of the let-7 small temporal RNA. *Science* **293**, 834–838 (2001).
17. Lee, C.Y., Lee, A. & Chanfreau, G. The roles of endonucleolytic cleavage and exonucleolytic digestion in the 5′-end processing of *S. cerevisiae* box C/D snoRNAs. *RNA* **9**, 1362–1370 (2003).
18. Nykänen, A., Haley, B. & Zamore, P.D. ATP requirements and small interfering RNA structure in the RNA interference pathway. *Cell* **107**, 309–321 (2001).
19. Chendrimada, T.P. *et al.* MicroRNA silencing through RISC recruitment of eIF6. *Nature* **447**, 823–828 (2007).
20. Chen, C. *et al.* Real-time quantification of microRNAs by stem-loop RT-PCR. *Nucleic Acids Res.* **33**, e179 (2005).
21. Modahl, L.E., MacNaughton, T.B., Zhu, N., Johnson, D.L. & Lai, M.M. RNA-dependent replication and transcription of hepatitis delta virus RNA involve distinct cellular RNA polymerases. *Mol. Cell. Biol.* **20**, 6030–6039 (2000).
22. Filipovska, J. & Konarska, M.M. Specific HDV RNA-templated transcription by Pol II in vitro. *RNA* **6**, 41–54 (2000).
23. Lehmann, E., Brueckner, F. & Cramer, P. Molecular basis of RNA-dependent RNA polymerase II activity. *Nature* **450**, 445–459 (2007).
24. Sato, S., Cornillez-Ty, C. & Lazinski, D.W. By inhibiting replication, the large hepatitis delta antigen can indirectly regulate amber/W editing and its own expression. *J. Virol.* **78**, 8120–8134 (2004).
25. Tavanez, J.P. *et al.* Hepatitis delta virus ribonucleoproteins shuttle between the nucleus and the cytoplasm. *RNA* **8**, 637–646 (2002).
26. Aoki, K., Moriguchi, H., Yoshioka, T., Okawa, K. & Tabara, H. *In vitro* analyses of the production and activity of secondary small interfering RNAs in *C. elegans*. *EMBO J.* **26**, 5007–5019 (2007).
27. Hornung, V. *et al.* 5′-Triphosphate RNA is the ligand for RIG-I. *Science* **314**, 994–997 (2006).
28. Cheng, J. *et al.* Transcriptional maps of 10 human chromosomes at 5-nucleotide resolution. *Science* **308**, 1149–1154 (2005).
29. Sureau, C., Guerra, B. & Lanford, R.E. Role of the large hepatitis B virus envelope protein in infectivity of the hepatitis delta virion. *J. Virol.* **67**, 366–372 (1993).
30. Haussecker, D. & Proudfoot, N.J. Dicer-dependent turnover of intergenic transcripts from the human beta-globin gene cluster. *Mol. Cell. Biol.* **25**, 9724–9733 (2005).
31. Gregory, R.I., Chendrimada, T.P. & Shiekhattar, R. MicroRNA biogenesis: isolation and characterization of the microprocessor complex. *Methods Mol. Biol.* **342**, 33–47 (2006).
32. Lau, N.C., Lim, L.P., Weinstein, E.G. & Bartel, D.P. An abundant class of tiny RNAs with probable regulatory roles in *Caenorhabditis elegans*. *Science* **294**, 858–862 (2001).
33. Parameswaran, P. *et al.* A pyrosequencing-tailored nucleotide barcode design unveils opportunities for large-scale sample multiplexing. *Nucleic Acids Res.* **35**, e130 (2007).
34. Kuo, M.Y. *et al.* Molecular cloning of hepatitis delta virus RNA from an infected woodchuck liver: sequence, structure, and applications. *J. Virol.* **62**, 1855–1861 (1988).

# Erratum: Capped small RNAs and *MOV10* in human hepatitis delta virus replication

**Dirk Haussecker, Dan Cao, Yong Huang, Poornima Parameswaran, Andrew Z Fire & Mark A Kay**

***Nat. Struct. Mol. Biol.* doi:10.1038/nsmb.1440; published online 15 June, corrected online 22 June 2008**

In the version of this article initially published online, the top panel in Figure 3d was mistakenly replaced with a panel from Figure 3c. The correct version of Figure 3d is shown below. The error has been corrected for all versions of this article.